Optica Applicata, Vol. LV, No. 2, 2025
DOI: 10.37190/oa/202343

Design and analysis of multi-angle diffraction efficiency distribution for all-dielectric transmissive grating

Jiaze Zhu[1], Huizhen Feng[2], Wenkang Huang[3], Jianfeng Xu[4], Ying Tian[1], Mian Jia[1], Manna Gu[2,*]

[1] Institute of Optoelectronic Technology, China Jiliang University, Hangzhou 310018, China

[2] College of Information Engineering, China Jiliang University, Hangzhou 310018, China

[3] Zhejiang Institute of Economics and Trade, Hangzhou 310018, China

[4] Special Equipment College, Hangzhou Vocational and Technical College, Hangzhou 310018, China

[*] Corresponding author: 154495791@qq.com

This paper presents the design of a C-shaped all-dielectric metasurface. The C-shaped dielectric structure and its substrate materials are Si and SiO_2, respectively. This unit structure enables independent control of the amplitude and phase of cross-polarized transmitted terahertz electromagnetic waves. By using parameter scanning method, four different unit structures were optimized at 0.1 and 1 THz, achieving unit phase distributions with a 45° interval within the range of 0° to 180°. Additionally, a 180° phase jump occurs when the unit structure rotates by 90°, achieving full phase control over the 360° range. By adjusting the orientation of the unit structure, arbitrary amplitude control can also be achieved. The highest transmission coefficients for the unit structures at 0.1 and 1 THz are 0.62 and 0.56, respectively. To verify the control capability of the designed unit structure on transmitted electromagnetic waves, metasurface gratings were designed based on these unit structures, enabling arbitrary control of diffraction angles and orders. At both frequencies, two different metasurface gratings were designed with diffraction orders of ($m = +1$) and ($m = +1, +3$). Near-field and far-field simulations of the super-grating structures were conducted using the finite integral method. The designed metasurface grating demonstrates effective control of cross-polarized transmitted waves, and its deflection angles conform to diffraction laws.

Keywords: optics, grating, metasurface.

1. Introduction

The study of metamaterials initially emerged in the field of electromagnetics. In 1967, Soviet physicist V.G. Veselago proposed a negative refractive index material with both negative permittivity and permeability, where the magnetic field, electric field, and wave vector formed a left-handed system. Pendry pointed out that electromagnetic waves in such materials would exhibit properties opposite to those of right-handed materials, such as negative Cherenkov effects, negative refraction, and anomalous Doppler effects [1-3]. However, due to the lack of naturally occurring negative refractive index materials, research on this concept remained theoretical for many years.

In 1996, British scientist J.B. Pendry proposed that negative permittivity and permeability could be achieved using metallic resonant rings and periodic metal strips, marking a turning point in the study of negative refractive index materials [1]. In 2001, D. Smith and his team at the University of California, San Diego, successfully fabricated a metamaterial with negative permeability and permittivity, experimentally verifying negative refraction and negative refractive index. In 2006, Professor J.B. Pendry theoretically confirmed the feasibility of negative refractive index materials and predicted their potential applications in perfect lenses, electromagnetic cloaking, and microwave beam focusing [3].

In 2006, Smith and his research team designed and fabricated an "invisibility cloak," which was successfully demonstrated experimentally. Around the same time, Professor John Pendry from Imperial College London independently proposed the concept of transformation optics and the design method for perfect cloaking devices [4]. Subsequently, Smith's team at Duke University completed experimental validation of the invisibility cloak.

In 2011, Capasso's research team introduced two-dimensional metamaterials, known as metasurfaces [5]. The introduction of metasurfaces addressed the limitations of three-dimensional metamaterials, opening a new chapter in metasurface research. In recent years, metasurfaces have attracted increasing attention due to their simple design, planar geometries, and excellent control over electromagnetic waves.

Researchers proposed a broadband metasurface using a metallic C-shaped structure as the unit structure [6-10], capable of simultaneously controlling electromagnetic wave amplitude and phase. The research group introduced the novel concept of coding metamaterials, enabling digital signal processing on metasurfaces to manipulate electromagnetic waves, thereby pioneering the field of information metamaterials. Researchers designed a metasurface based on high-resistance silicon to control the transmission phase and amplitude of terahertz waves and further developed an exotic grating for testing, capable of arbitrarily controlling diffraction orders [11-20].

Since its inception, metasurface research has demonstrated unique electromagnetic properties and facilitated the development of ultra-thin optical devices, such as meta -lenses, cloaking devices, and holographic plates [21-35]. Although metasurface research and applications are still in their early stages worldwide, their future potential is immense [36-50].

This paper primarily focuses on designing two groups of all-dielectric unit structures using dielectric materials. The C-shaped structures use Si as the primary material and SiO_2 as the substrate. These unit structures achieve full phase control of cross

-polarized transmitted terahertz electromagnetic waves at 0.1 and 1 THz frequencies. Each frequency requires four unit structures to achieve 2π phase control of the transmitted cross-polarized waves. By rotating the unit structures, different amplitude controls can be obtained. To verify the control capability of the designed unit structures, the four unit structures were arranged in specific patterns to create metasurface gratings capable of controlling different diffraction orders. Based on transmission theory, the phase and amplitude distribution of the desired diffraction order gratings were determined, and the geometric parameters and orientation of the C-shaped unit structures were optimized accordingly. The designed metasurface gratings were simulated using the finite integral method to obtain near-field and far-field distributions. The simulation results confirmed their capability to control cross-polarized transmitted terahertz waves.

2. Unit structure design

The designed unit structure has two functional types: phase control is determined by the geometric shape of each unit structure, while amplitude control is achieved through the rotation angle of the unit structure. The C-shaped structure uses high-resistance silicon as the dielectric material with the substrate made of dielectric material.

Figure 1 shows the designed unit structure with a base period of t and a height of h_s. The height of the C-shaped structure is h, the inner radius is r_n, the outer radius is r_w, the opening size is α, and the angle between the central axis of the opening angle and the x-axis is β, which is the rotation angle of the structural unit, as shown in Fig. 2. The electromagnetic wave is incident on the unit structure on the C-type structure side. The C-type structure is composed of a high-resistance silicon material with a dielectric constant of 11.9. The base material is silicon dioxide with a refractive index of 1.46. When a linearly polarized plane wave is incident on a C-type unit structure, both symmetric E_s mode and asymmetric E_{as} mode are excited simultaneously, and the scattering

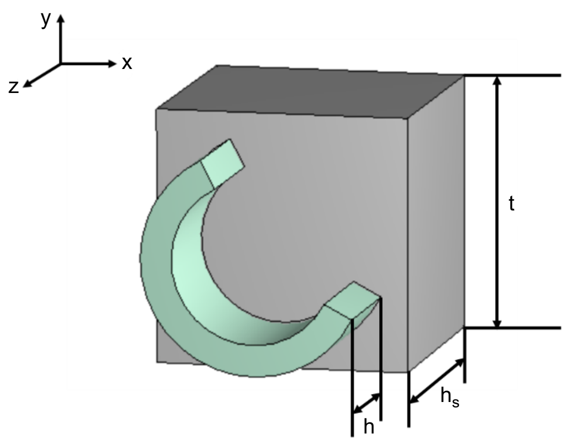

Fig. 1. Schematic diagram of the unit structure.

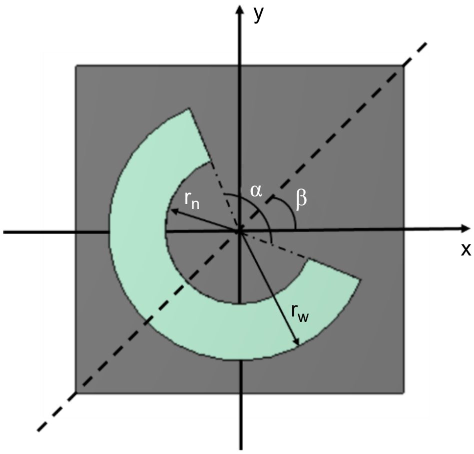

Fig. 2. Front view of the unit structure.

fields of the two modes form orthogonally polarized transmitted waves. By designing the geometric shape and opening size of the unit structure, the polarization of the transmitted light is orthogonal to that of the incident light with a phase difference of 180°. The designed unit structure achieves maximum conversion efficiency of linear polarization at $\beta = 45°$ and $\beta = -45°$. At this point, the incident y-polarized wave is efficiently converted into x-polarized transmitted wave. When the y-polarized wave E_y is incident on the designed C-type unit structure, the law of the y-polarized transmitted wave formed is [5]

$$E_y^{\mathrm{s}} = \frac{1}{2} E_y^{\mathrm{i}} \sin(2\beta) \sum_{n=1}^{4} A_n \exp(i\varphi_n) \tag{1}$$

In the equation, E_y^{i} is the incoming y-polarized wave, and A_n and φ_n are the scattering amplitude and phase of the n-th resonant mode with $\beta = 45°$. We will design two types of unit structures at frequencies of 0.1 and 1 THz, respectively. Due to the phase transition of π in the unit structure at $\beta = 0°$, four different structural parameters with a phase difference of 45° and polarization conversion are selected at each frequency to achieve full phase control of cross-polarized transmitted electromagnetic waves. By rotating their unit structures, different transmission coefficients can be obtained.

By using the finite integration method, the designed microstructure element was simulated and optimized continuously. We used the parameter scanning method to optimize the geometric parameters of the element structure. For the element structure at 0.1 THz, $t = 1800$ μm was obtained through optimization of parameters, $h = 900$ μm, and $h_s = 1000$ μm. For the unit structure at 1 THz, the optimized result is $t = 180$ μm, $h = 90$ μm, and $h_s = 200$ μm. Other specific parameters are shown in Tables 1 and 2. In the numerical simulation of cell structures, we used periodic boundary conditions. In the process of calculating the whole structure, we used open boundary conditions.

Figures 3 and 4 show the calculation results of the cross-polarization transmission coefficient and phase change when the opening angle α changes. It can be seen that

T a b l e 1. Specific parameter table of unit structure at 0.1 THz.

Parameters	Unit cell			
	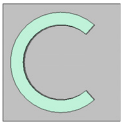	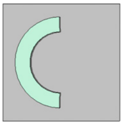	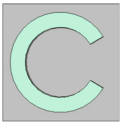	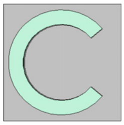
r_n	570	465	532	578
r_w	760	691	760	800
α	97	183	62	80
Amplitude	(0, 0.770)	(0, 0.628)	(0, 0.758)	(0, 0.761)
Phase	25° (–155°)	70° (–110°)	115° (–65°)	160° (–20°)

T a b l e 2. Specific parameter table of unit structure at 1 THz.

Parameters	Unit cell			
				
r_n	46.2	42.5	43.7	41.6
r_w	67	62.7	66.8	63.2
α	90	85	70	65
Amplitude	(0, 0.586)	(0, 0.569)	(0, 0.580)	(0, 0.577)
Phase	25° (–155°)	70° (–110°)	115° (–65°)	160° (–20°)

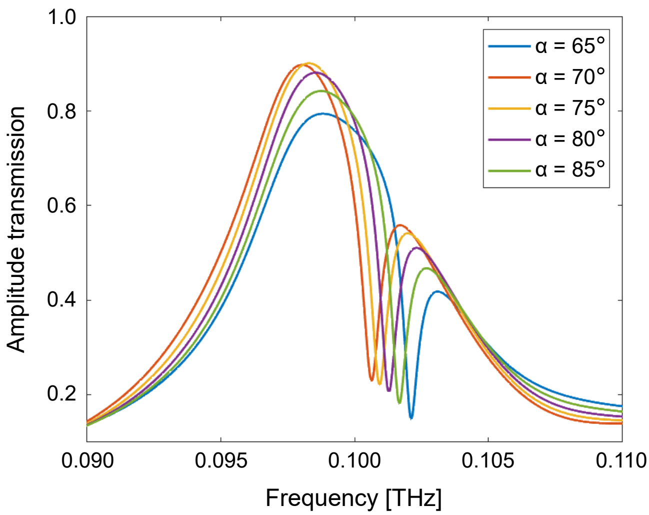

Fig. 3. The transmission coefficient variation curve of changing the opening angle α.

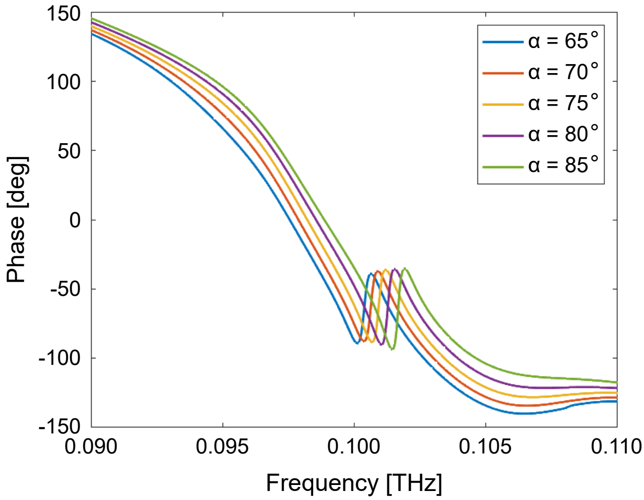

Fig. 4. The phase curve of the opening angle α.

when $\beta = 45°$ remains constant, changing the opening angle α of the C-type structure can alter the phase of the cross-polarized transmitted wave, while the amplitude can remain approximately constant within a certain bandwidth. The appropriate phase of the unit structure can be optimized by adjusting the value of the opening angle α of the C-type structure unit.

Figures 5 and 6 respectively show the cross-polarization transmission coefficient and phase change by rotating the orientation angle β of the C-type structure. Changing the rotation angle β of the C-type structure not only causes a phase transition of π at 0°, but also maintains the phase of the cross-polarized transmitted light approximately

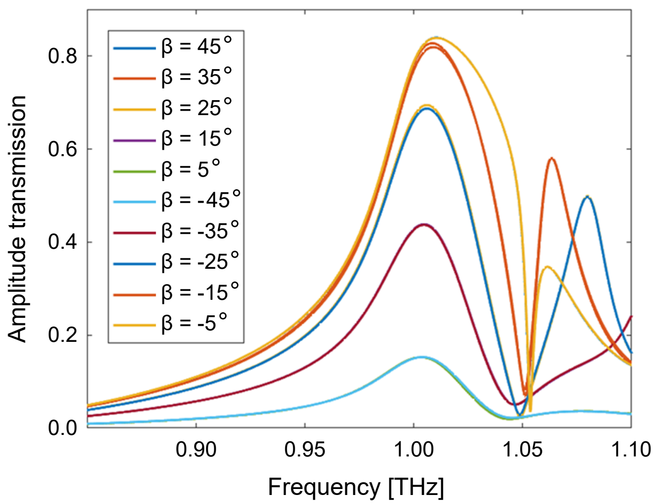

Fig. 5. The transmission coefficient curve by changing the rotation angle β.

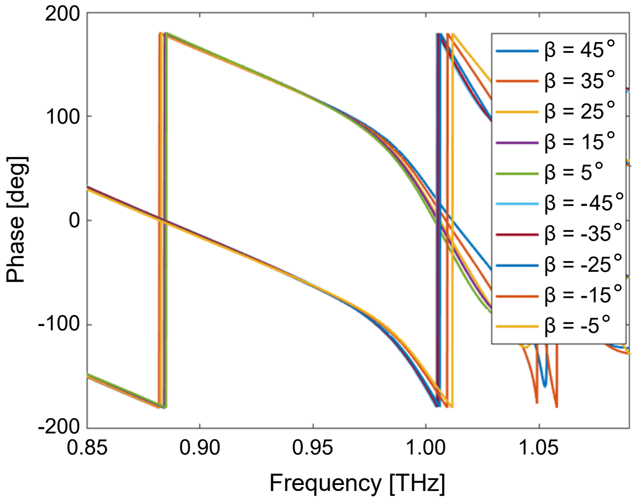

Fig. 6. The phase change curve of the rotation angle β.

unchanged at the corresponding frequency. That is, the changing the orientation angle of the C-type structure has little effect on the phase change of its cross-polarized transmitted terahertz waves, while its transmission coefficient decreases continuously with the decrease of the absolute value of β when the orientation angle changes between (0°, 45°) or (0°, –45°).

3. Design of metasurface gratings

In order to achieve simultaneous control of the amplitude and phase of cross-polarized transmitted light using the above method, this paper designs a metasurface grating composed of an optimized all dielectric C-type unit structure arrangement, which can achieve arbitrary control of the diffraction order and number of cross-polarized transmitted light at corresponding frequencies. When the incident light passes through the interface, the transmission distribution coefficient of the cross-polarized transmitted light can be expressed as [9]

$$t(x) = A(x)\exp\left[i\varphi(x)\right] = \sum_m A_m \exp\left(\frac{-i2m\pi x}{d}\right) \tag{2}$$

Among them, $A(x)$ and $\varphi(x)$ respectively represent the amplitude distribution and phase distribution transmitted through the grating, d is the grating period, x represents the position, and m is the diffraction order. In order to generate multiple diffraction orders, it is necessary to simultaneously control the amplitude and phase of the grating.

We designed two types of gratings at both 0.1 and 1 THz, each consisting of four different geometric unit structures with uniform phase distribution at (0, π). As the sign of the C-type structure orientation angle β changes, a phase transition of π can be in-

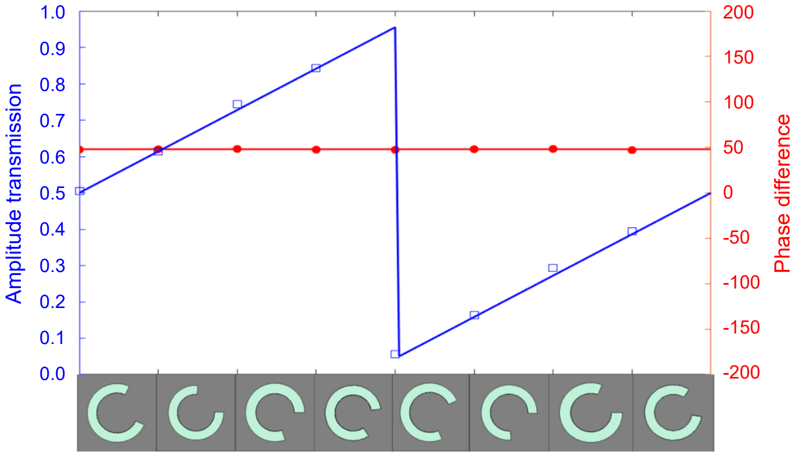

Fig. 7. Transmission coefficient and phase distribution of cross-polarized transmitted waves at 0.1 THz ($m = +1$).

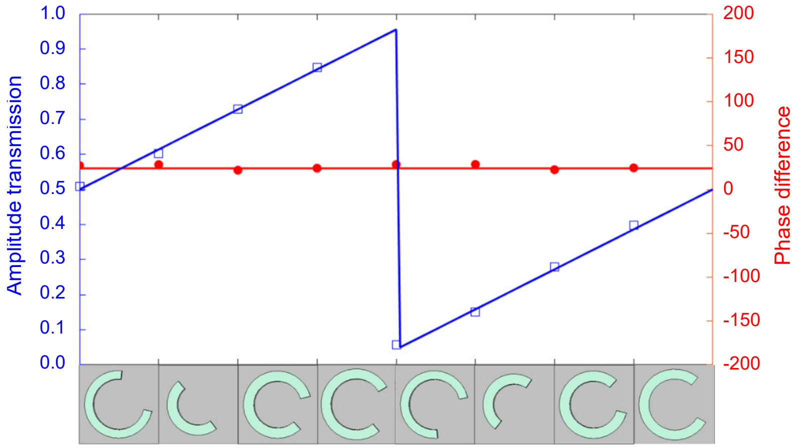

Fig. 8. Transmission coefficient and phase distribution of cross-polarized transmitted waves at 1 THz ($m = +1$).

troduced, achieving control over the phase at $(0, 2\pi)$. We can arrange the four types of unit structures in equidistant and discrete patterns to obtain gratings with ($m = +1$) diffraction orders, as shown in Figs. 7 and 8. The solid line in the figure represents the theoretical result obtained from the grating transmission formula (2), and the circle and squares represent the simulation results of the amplitude and phase corresponding to the designed unit structure.

As shown in Figs. 7 and 8, the metasurface grating that produces a single diffraction order ($m = +1$) consists of 8 unit structures to achieve uniform amplitude distribution and continuous phase distribution at $(0, 2\pi)$. It can be observed that when only +1-order diffraction exists, the amplitude distribution of the transmitted cross-polarized wave

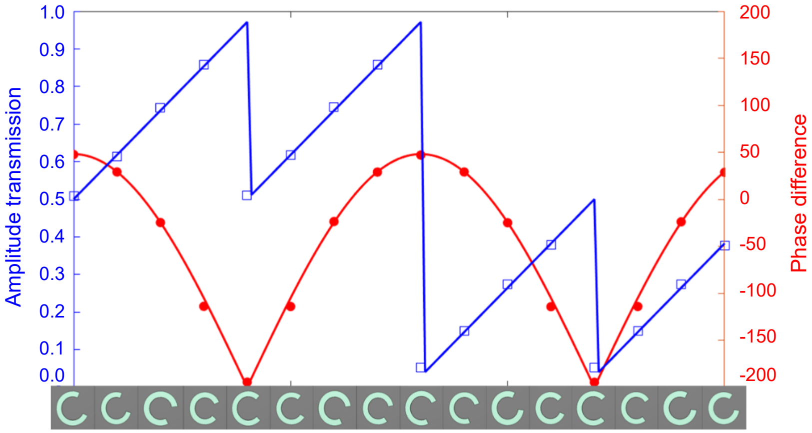

Fig. 9. Transmission coefficient and phase distribution of cross-polarized transmitted waves at 0.1 THz (m = +1,+3).

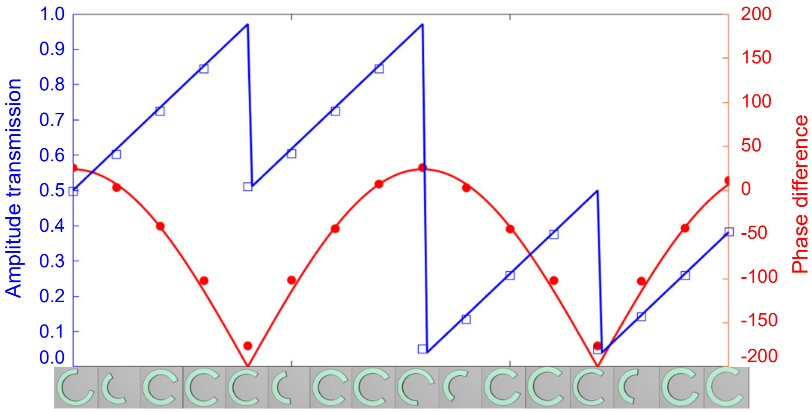

Fig. 10. Transmission coefficient and phase distribution of cross-polarized transmitted waves at 1 THz (m = +1,+3).

is uniform, with amplitudes of 0.62 and 0.56 at 0.1 and 1 THz, respectively. The phase distribution varies linearly and is uniformly distributed within (0, 2π). Designed gratings with (m = +1, +3) diffraction orders are shown in Figs. 9 and 10.

From Figs. 9 and 10, it can be observed that the metasurface grating produces multiple diffraction orders. In order to achieve the desired phase and amplitude distribution, the orientation angle β of the unit structures continuously varies within the range of (0, 2π). When it is a (+1, +3)-order diffraction, due to mutual superposition, the distribution of phase and amplitude of the cross-polarized transmitted wave is no longer uniform. The simulation results of the designed unit structure show good agreement between the amplitude and phase distributions and the theoretically calculated distributions.

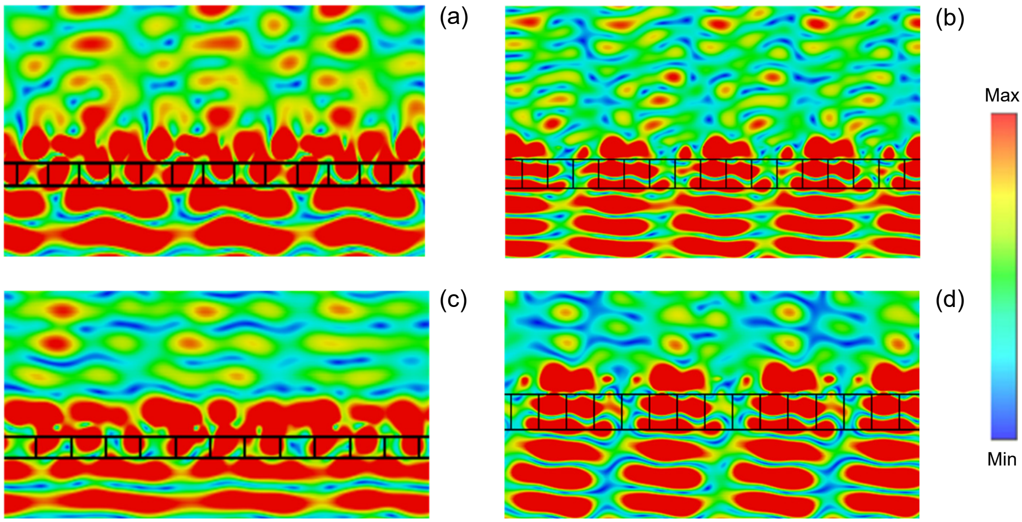

Fig. 11. The near-field mode simulation results of ($m = +1$)-order diffraction at (a) 0.1 THz and (b) 1 THz. The near-field mode simulation results of ($m = +1,+3$)-order diffraction at (c) 0.1 THz and (d) 1 THz.

The time-domain solver was used to simulate the designed metasurface grating, and the simulation results in near-field mode are shown in Fig. 11. As shown in Fig. 11, in the near-field, it can be observed that the transmitted wavefront has a certain deviation compared to the incident wavefront, proving that the designed metasurface grating has a certain regulatory effect on the transmitted cross-polarized terahertz waves. However, in the near-field mode simulation results, the deflection angle of the wavefront is not clear, and its deflection angle can be solved by the grating equation, that is:

$$d \sin\theta = m\lambda \tag{3}$$

Therefore, the deflection angle θ can be expressed as

$$\theta = \arcsin\frac{m\lambda}{d} \tag{4}$$

It can be calculated that for the frequency of 0.1 THz, the diffraction angle of the (+1)-order grating is 12°, and the diffraction angles of the (+1, +3)-order gratings are 6° and 18°, respectively.

The far-field mode can be clearly observed with the deflection angle of the wavefront. Some side lobes appear in the far-field scattering characteristics, which may be caused by the insufficient size of the overall structure we calculated. If we increase the overall size of the device, these sidelobes may decrease. The simulation results of the far-field mode of the transmitted cross-polarized (*i.e.* x-polarized) waves are shown in Fig. 12 with the y-polarized incidence. As shown in Fig. 12, compared with the simulation results of near-field mode, it can be clearly seen that the deflection angle of ($m = +1$)-order diffraction transmitted cross-polarized waves is 12°, and the deflection

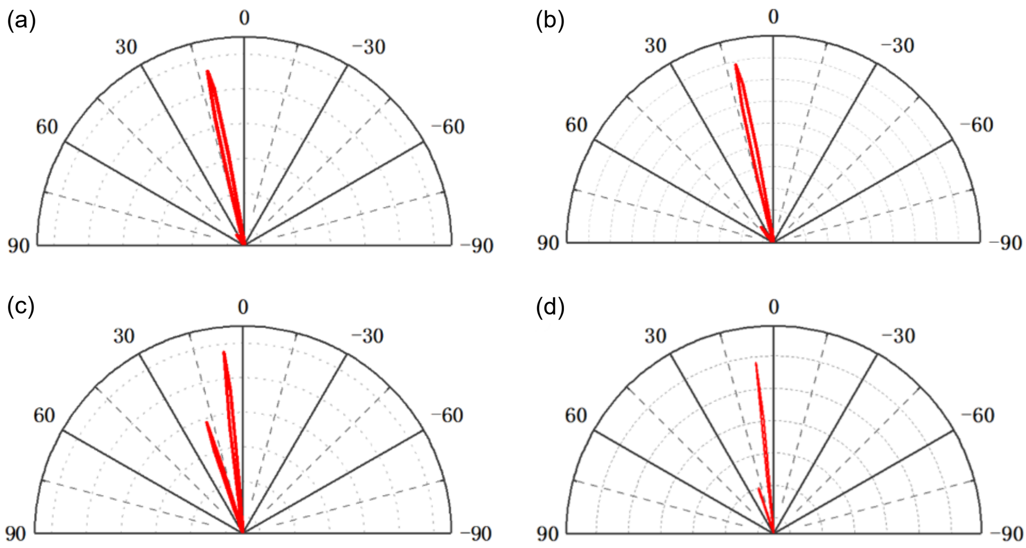

Fig. 12. The far-field mode simulation results of (m = +1)-order diffraction at (a) 0.1 THz and (b) 1 THz. The far-field mode simulation results of (m = +1, +3)-order diffraction at (c) 0.1 THz and (d) 1 THz.

angles of (m = +1,+3)-order diffraction transmitted cross-polarized waves are 6° and 18°, respectively. In the far-field patterns of (m = +1, +3)-order diffraction, the transmission coefficients of (m = +1)-order diffraction at 0.1 and 1 THz are higher than those of (m = +3)-order diffraction, which conforms to the energy distribution law of grating diffraction. Therefore, the metasurface grating designed in this article can achieve modulation of transmitted terahertz electromagnetic waves at 0.1 and 1 THz.

Even though the presented work is fully based on numerical simulations of metasurface grating, it is feasible to prepare such all dielectric metasurfaces. Since the designed all-dielectric metasurface is in the terahertz band, the fabrication of such large depth metasurface microstructure may not be possible using conventional lithographic processes [51]. Firstly, a layer of silica should be deposited on a thick high resistivity silicon wafer by using chemical vapor deposition. The wafer should be then directly bonded with a fused silica substrate. The conventional mask photolithography can be applied to form a pattern of square array on the layer of silica with photoresist. The layer of silica should be removed by C_4F_8 gas, and the remaining pattern should be kept as a protection mask for subsequent etching. Next, the Bosch process by using deep reactive ion etching technique should be used to etch the silicon wafer, and the Bosch process should be repeated until the silicon is completely removed.

4. Conclusion

This article proposes an all dielectric C-type unit structure. This structure can be used to simultaneously control the amplitude and phase of transmitted cross-polarized terahertz electromagnetic waves. By adjusting the geometric parameters of the C-type structure and the relative spectral position of the geometric resonance, two types of unit structures were designed at 0.1 and 1 THz, respectively. Each type of unit structure contains four types of unit structures with equivalent polarization conversion ability and different geometric parameters. Its characteristic is that the transmission phase difference between adjacent unit structures is 45°, and combined with changing the orientation angle, a sudden change of 180° phase difference can be obtained to achieve full phase control of transmitted cross-polarized waves. By rotating the orientation angle of the designed unit structure, different cross-polarized transmission amplitudes can be obtained. The highest transmission coefficients of the designed unit structure at 0.1 and 1 THz are 0.62 and 0.56, respectively. Therefore, by designing two types of unit structures and rotating their orientation angles, complete control of transmitted waves can be achieved. This artificially designed all dielectric metamaterial is simple in design, easy to process, and has less loss compared to metal materials. All dielectric metasurface designed provides an efficient and convenient method for controlling terahertz wavefront.

Acknowledgement
Natural Science Foundation of Zhejiang Province (No. LZ21A040003, No. LY20F050007).

Data availability
The data that support the findings of this study are available from the corresponding author upon reasonable request.

References

[1] PENDRY J.B., HOLDEN A.J., STEWART W.J., YOUNGS I., *Extremely low frequency plasmons in metallic mesostructures*, Physical Review Letters **76**(25), 1996: 4773. https://doi.org/10.1103/PhysRevLett.76.4773

[2] SHELBY R.A., SMITH D.R., SCHULTZ S., *Experimental verification of a negative index of refraction*, Science **292**(5514), 2001: 77-79. https://doi.org/10.1126/science.1058847

[3] SCHURIG D., MOCK J.J., JUSTICE B.J., CUMMER S.A., PENDRY J.B., STARR A.F., SMITH D.R., *Metamaterial electromagnetic cloak at microwave frequencies*, Science **314**(5801), 2006: 977-980. https://doi.org/10.1126/science.1133628

[4] ZHAO Q., ZHOU J., ZHANG F., LIPPENS D., *Mie resonance-based dielectric metamaterials*, Materials Today **12**(12), 2009: 60-69. https://doi.org/10.1016/S1369-7021(09)70318-9

[5] YU N., GENEVET P.,KATS M.A., AIETA F., TETIENNE J.-P., CAPASSO F., GABURRO Z., *Light propagation with phase discontinuities: Generalized laws of reflection and refraction*, Science **334**(6054), 2011: 333-337. https://doi.org/10.1126/science.1210713

[6] SOUKOULIS C.M., WEGENER M., *Past achievements and future challenges in the development of three -dimensional photonic metamaterials*, Nature Photonics **5**(9), 2011: 523-530. https://doi.org/10.1038/nphoton.2011.154

[7] ZHANG X., TIAN Z., YUE W., GU J., ZHANG S., HAN J., ZHANG W., *Broadband terahertz wave deflection based on C-shape complex metamaterials with phase discontinuities*, Advanced Materials **25**(33), 2013: 4567-4572. https://doi.org/10.1002/adma.201204850

[8] GRADY N.K., HEYES J.E., CHOWDHURY D.R., ZENG Y., REITEN M.T., AZAD A.K., TAYLOR A.J., DALVIT D.A.R., CHEN H.-T., *Terahertz metamaterials for linear polarization conversion and anomalous refraction*, Science **340**(6138), 2013: 1304-1307. https://doi.org/10.1126/science.1235399

[9] Liu L., Zhang X., Kenney M., Su X., Xu N., Ouyang C., Shi Y., Han J., Zhang W., Zhang S., *Broadband metasurfaces with simultaneous control of phase and amplitude*, Advanced Materials **26**(29), 2014: 5031-5036. https://doi.org/10.1002/adma.201401484

[10] Akram M.R., Ding G., Chen K., Feng Y., Zhu W., *Ultrathin single layer metasurfaces with ultra-wideband operation for both transmission and reflection*, Advanced Materials **32**(12), 2020: 1907308. https://doi.org/10.1002/adma.201907308

[11] Huang L., Chen X., Mühlenbernd H., Zhang H., Chen S., Bai B., Tan Q., Jin G., Cheah K.-W., Qiu C.-W., Li J., Zentgraf T., Zhang S., *Three-dimensional optical holography using a plasmonic metasurface*, Nature Communications **4**, 2013: 2808. https://doi.org/10.1038/ncomms3808

[12] Jia S.L., Wan X., Su P., Zhao Y.J., Cui T.J., *Broadband metasurface for independent control of reflected amplitude and phase*, AIP Advances **6**(4), 2016: 045024. https://doi.org/10.1063/1.4948513

[13] Forouzmand A., Mosallaei H., *All-dielectric C-shaped nanoantennas for light manipulation: Tailoring both magnetic and electric resonances to the desire*, Advanced Optical Materials **5**(14), 2017: 1700147. https://doi.org/10.1002/adom.201700147

[14] Akram M.R., Bai X., Jin R., Vandenbosch G.A.E., Premaratne M., Zhu W., *Photon spin Hall effect-based ultra-thin transmissive metasurface for efficient generation of OAM waves*, IEEE Transactions on Antennas and Propagation **67**(7), 2019: 4650-4658. https://doi.org/10.1109/TAP.2019.2905777

[15] Li J., Jin R., Geng J., Liang X., Wang K., Premaratne M., Zhu W., *Design of a broadband metasurface Luneburg lens for full-angle operation*, IEEE Transactions on Antennas and Propagation **67**(4), 2019: 2442-2451. https://doi.org/10.1109/TAP.2018.2889006

[16] Zhang C., Xue T., Zhang J., Li Z., Liu L., Xie J., Yao J., Wang G., Ye X., Zhu W., *Terahertz meta-biosensor based on high-Q electrical resonance enhanced by the interference of toroidal dipole*, Biosensors and Bioelectronics **214**, 2022: 114493. https://doi.org/10.1016/j.bios.2022.114493

[17] Zhang C., Xue T., Zhang J., Liu L., Xie J., Wang G., Yao J., Zhu W., Ye X., *Terahertz toroidal metasurface biosensor for sensitive distinction of lung cancer cells*, Nanophotonics **11**(1), 2022: 101-109. https://doi.org/10.1515/nanoph-2021-0520

[18] Zhang J., Mu N., Liu L., Xie J., Feng H., Yao J., Chen T., Zhu W., *Highly sensitive detection of malignant glioma cells using metamaterial-inspired THz biosensor based on electromagnetically induced transparency*, Biosensors and Bioelectronics **185**, 2021: 113241. https://doi.org/10.1016/j.bios.2021.113241

[19] Istokskaia V., Lefebvre B., Versaci R., Dreghici D.B., Doria D., Grepl F., Olšovcová V., Schillaci F., Stanček S., Tryus M., Velyhan A., Margarone D., Giuffrida L., *Real-time bremsstrahlung detector as a monitoring tool for laser–plasma proton acceleration*, High Power Laser Science and Engineering **12**, 2024: e57. https://doi.org/10.1017/hpl.2024.38

[20] Peters C., Forbes A., *Controlling the hidden parity in vectorial light with metasurfaces*, Advanced Photonics **6**(4), 2024: 040501. https://doi.org/10.1117/1.AP.6.4.040501

[21] Shi J., Yang C., Chen Y., Wang T., Yu H., Cao J., Geng Z., Wang Z., Wen H., Tan H., Zhang Y., Jiang D., Wu D., Xu Y., Ni H., Niu Z., *Precise mode control of mid-infrared high-power laser diodes using on-chip advanced sawtooth waveguide designs*, High Power Laser Science and Engineering **12**, 2024: e42. https://doi.org/10.1017/hpl.2024.23

[22] Ullah M., Mikki S., *Optical nonreciprocity in a multimode cavity optomechanical system controlled by dynamic Casimir force*, Advanced Quantum Technologies **7**(7), 2024: 2400007. https://doi.org/10.1002/qute.202400007

[23] Zhang C.-L., Hu K.-X., Zhang J., Cao J., Zhang S., Wang H.-F., *Topological phase transition and edge states with tunable localization in the cyclic four-mode optical system*, Advanced Quantum Technologies **7**(10), 2024: 2400165. https://doi.org/10.1002/qute.202400165

[24] Seo J., Jo J., Kim J., Kang J., Kang C., Moon S.-W., Lee E., Hong J., Rho J., Chung H., *Deep-learning-driven end-to-end metalens imaging*, Advanced Photonics **6**(6), 2024: 066002. https://doi.org/10.1117/1.AP.6.6.066002

[25] LUO Z.Y., DING Y.Q., PENG F.L., WEI G.H., WANG Y., WU S.-T., *Ultracompact and high-efficiency liquid-crystal-on-silicon light engines for augmented reality glasses*, Opto-Electronic Advances **7**, 2024: 240039. https://doi.org/10.29026/oea.2024.240039

[26] LI S.S., FANG Y.N., WANG J.F., *Control of light–matter interactions in two-dimensional materials with nanoparticle-on-mirror structures*, Opto-Electronic Science **3**, 2024: 240011. https://doi.org/10.29026/oes.2024.240011

[27] LIANG M.W., LU D.Z., MA Y.G., *Vectorial optical fields manipulation via metasurfaces*, Opto-Electronic Engineering **51**(8), 2024: 240068. https://doi.org/10.12086/oee.2024.240068

[28] ZHANG S.X., LI H., FAN C.Z., ZENG Z.C., XIONG C., WU J., YAN Z.J., LIU D.M., SUN Q.Z., *Adaptive decentralized AI scheme for signal recognition of distributed sensor systems*, Opto-Electronic Advances **7**, 2024: 240119. https://doi.org/10.29026/oea.2024.240119

[29] TAHA B.A., ADDIE A.J., HAIDER A.J., CHAUDHARY V., APSARI R., KAUSHIK A., ARSAD N., *Exploring trends and opportunities in quantum-enhanced advanced photonic illumination technologies*, Advanced Quantum Technologies **7**(3), 2024: 2300414. https://doi.org/10.1002/qute.202300414

[30] RANE S., PRABHU S., CHOWDHURY D.R., *Physics and applications of terahertz metagratings*, Opto -Electronic Science **3**, 2024: 230049. https://doi.org/10.29026/oes.2024.230049

[31] ZHOU L., LOU H., DENG Z., QIN X., PAN J., DI Y., GU C., LUO D., LI W., *Compact mid-infrared dual-comb spectrometer over 3–4 μm via intra-pulse difference frequency generation in $LiNbO_3$ waveguides*, High Power Laser Science and Engineering **12**, 2024: e23. https://doi.org/10.1017/hpl.2024.2

[32] RAHMAN M.S.S., OZCAN A., *Physics and artificial intelligence: illuminating the future of optics and photonics*, Advanced Photonics **6**(5), 2024: 050500. https://doi.org/10.1117/1.AP.6.5.050500

[33] REFAELI Z., MARCUS G., SHAMIR Y., *A simple method for pulse contrast enhancement via self-focusing*, High Power Laser Science and Engineering **12**, 2024: e18. https://doi.org/10.1017/hpl.2023.99

[34] SHEN C.-Y., LI J., LI Y., GAN T., BAI L., JARRAHI M., OZCAN A., *Multiplane quantitative phase imaging using a wavelength-multiplexed diffractive optical processor*, Advanced Photonics **6**(5), 2024: 056003. https://doi.org/10.1117/1.AP.6.5.056003

[35] YANG H., HE H.R., HU Y.Q., DUAN H.G., *Metasurface-empowered vector light field regulation, detection and application*, Opto-Electronic Engineering **51**(8), 2024: 240168. https://doi.org/10.12086/oee.2024.240168

[36] WU Y.C., YANG Q.P., SHEN B.T., TAO Y.S., ZHANG X.G., TAO Z.H., XING L.W., GE Z.F., LI T.T., BAI B.W., SHU H.W., WANG X.J., *Multifunctional mixed analog/digital signal processor based on integrated photonics*, Opto-Electronic Science **3**, 2024: 240012. https://doi.org/10.29026/oes.2024.240012

[37] ABDELALL N., ALMOKHTAR M., KHOUQEER G., ABOOD I., EL. SOLIMAN S., *Rainbow trapping with engineered topological corner states and cavities in photonic crystals*, Advanced Quantum Technologies **7**(9), 2024: 2400050. https://doi.org/10.1002/qute.202400050

[38] LIU S., CAO W., JIANG S., HE L., LIN F., HE X., *3D Dirac semimetal supported tunable multi-frequency terahertz metamaterial absorbers*, Advanced Quantum Technologies **7**(4), 2024: 2300386. https://doi.org/10.1002/qute.202300386

[39] YU Z.J., LI M.X., XING Z.Y., GAO H., LIU Z.Y., PU S.L., MAO H., CAI H., MA Q., REN W.Q., ZHU J., ZHANG C., *Genetic algorithm assisted meta-atom design for high-performance metasurface optics*, Opto-Electronic Science **3**, 2024: 240016. https://doi.org/10.29026/oes.2024.240016

[40] WANG H.X., HE Y.L., ZHU H.W., DONG H., WANG S., *Research progress and prospects of metasurface polarization devices*, Opto-Electronic Engineering **51**(8), 2024: 240095. https://doi.org/10.12086/oee.2024.240095

[41] ZHANG J.C., CHEN M.K., FAN Y.B., CHEN Q.M., CHEN S.F., YAO J., LIU X.Y., XIAO S.M., TSAI D.P., *Miniature tunable Airy beam optical meta-device*, Opto-Electronic Advances **7**, 2024: 230171. https://doi.org/10.29026/oea.2024.230171

[42] ZHANG Y.N., CHEN Y.G., WANG T., ZHU Q., GU M., *Ultrahigh performance passive radiative cooling by hybrid polar dielectric metasurface thermal emitters*, Opto-Electronic Advances **7**, 2024, 230194. https://doi.org/10.29026/oea.2024.230194

[43] BERHE A.M., AS'HAM K., AL-ANI I., HATTORI H.T., MIROSHNICHENKO A.E., *Strong coupling and catenary field enhancement in the hybrid plasmonic metamaterial cavity and TMDC monolayers*, Opto-Electronic Advances **7**, 2024: 230181. https://doi.org/10.29026/oea.2024.230181

[44] NAN T., ZHAO H., GUO J.Y., WANG X.K., TIAN H., ZHANG Y., *Generation of structured light beams with polarization variation along arbitrary spatial trajectories using tri-layer metasurfaces*, Opto-Electronic Science **3**, 2024: 230052. https://doi.org/10.29026/oes.2024.230052

[45] JING X., GUI X., ZHOU P., HONG Z., *Physical explanation of Fabry–Pérot cavity for broadband bilayer metamaterials polarization converter*, Journal of Lightwave Technology **36**(12), 2018: 2322-2327. https://doi.org/10.1109/JLT.2018.2808339

[46] ZHAO J., JING X., WANG W., TIAN Y., ZHU D., SHI G., *Steady method to retrieve effective electromagnetic parameters of bianisotropic metamaterials at one incident direction in the terahertz region*, Optics & Laser Technology **95**, 2017: 56-62. https://doi.org/10.1016/j.optlastec.2017.04.001

[47] WANG Q.Y., LI C.X., FANG B., KE L., LU J.X., MA X.L., HONG Z., JING X.F., *Flexible and independent control of asymmetric vortex beams based on spin multiplexing all dielectric metasurface*, Journal of Lightwave Technology **41**(23), 2023: 7098-7104. https://doi.org/10.1109/JLT.2023.3238389

[48] ZENG B.W., LI C.X., CHENG H.L., FANG B., LU J.X., MA X.L., WANG L., HONG Z., JING X.F., *Anisotropic programmable metasurface beam splitter based on diode real-time control*, Optics and Lasers in Engineering **169**, 2023: 107723. https://doi.org/10.1016/j.optlaseng.2023.107723

[49] QIN G.H., DONG Y.Y., ZHANG P., LIU J.J., LI C.X., HUANG W.K., HONG Z., SHEN C.Y., JING X.F., *Broadband absorber coupled with anti-reflection inverted pyramid type all-dielectric microstructure*, Optics and Lasers in Engineering **160**, 2023: 107288. https://doi.org/10.1016/j.optlaseng.2022.107288

[50] JING X.F., TANG X.Y., TIAN Y., KONG Z., LI C.X., SHEN C.Y., HONG Z., *Enhancement of diffraction efficiency based on the addition principle of coded digital gratings*, Journal of Lightwave Technology **40**(1), 2022: 136-142. https://doi.org/10.1109/JLT.2021.3119380

[51] MA Z., HANHAM S.M., ALBELLA P., NG B., LU H.T., GONG Y., MAIER S.A., HONG M., *Terahertz all-dielectric magnetic mirror metasurfaces*, ACS Photonics **3**(6), 2016: 1010-1018. https://doi.org/10.1021/acsphotonics.6b00096

Received January 10, 2025
in revised form February 12, 2025